International Journal of Advanced Engineering Research and Science (IJAERS)
Peer-Reviewed Journal
ISSN: 2349-6495(P) | 2456-1908(O)
Vol-11, Issue-1; Jan, 2024
Journal Home Page Available: https://ijaers.com/
Article DOI: https://dx.doi.org/10.22161/ijaers.11.1

Fabrication of pure porous CuO from microwave-synthesized MOF-199 by calcination in ambient air

Nam Ho Phung Khac

Institute of Chemistry and Materials, No. 17 Hoang Sam Street, Cau Giay District, Ha Noi, Vietnam
*Email: homyhu@gmail.com

Received: 17 Nov 2023,

Receive in revised form: 25 Dec 2023,

Accepted: 02 Jan 2024,

Available online: 08 Jan 2024

***Keywords*— Copper (II) oxide, MOF-199, calcination process, oxidation catalysis.**

***Abstract*—** *Metal-organic frameworks with porous characteristics are applied in many fields. This study used it as a superior raw material source for making transition metal oxides. By calcining the copper 1,3,5-benzene tricarboxylate framework in ambient air, copper(II) oxide was produced. The calcination temperature was investigated in the range of 250 to 700 °C. At a calcination temperature of 550 °C, the resultant CuO has a homogeneous size and shape within the 1-2 um range. CuO's surface area of 33.16 m^2/g is more excellent than several other materials and technologies used in CuO manufacture. Utilizing CuO generated by the MOF-199 calcination process for enhanced oxidation catalysis in treating organic gases and vapors is based on the research findings.*

I. INTRODUCTION

Metal-organic framework materials are formed from metal ions or clusters and organic ligands, so they are diverse in structure, quantity, and type. This combination has brought many superior properties to the material, such as porosity, flexibility, combination ability, and applicability. With unique features, metal-organic framework materials have been applied in many fields, such as gas production [1-4], environmental treatment [5-7], energy storage and conversion [8-10], medicine [11-13], etc. Copper(II) benzene tricarboxylate is a metal-organic framework material formed from Cu^{2+} ions with 1,3,5-benzene tricarboxylate ligands. Cu-BTC has a regular octahedral structure and changes size according to synthesis conditions. Its' surface area ranges from 350 m^2/g to 1,800 m^2/g [14-17]. Pure and composite materials based on Cu-BTC are applied in fields such as CO_2 capture [16], H_2 adsorption [15], waste treatment [18], chemical catalysis [14, 19], sensors [20], etc. Cu-BTC is also used as a raw material to manufacture CuO_x as a catalyst for metabolic reactions such as selective reduction reactions [21] and electrochemical decomposition [22]. CuO_x made from Cu-BTC is also used as a NO_2 sensor [23], an electrochemical sensor [24], and a supercapacitor [25].

II. EXPERIMENTS

2.1. Chemical

1,3,5-Trimesic Acid (≥99%, H_3BTC), Copper (II) chloride dihydrate (≥99%, $CuCl_2.2H_2O$), ethanol (≥98%, C_2H_5OH), Dimethylformamide (≥99%, DMF) were purchased from Macklin Co. Ltd.

2.2. Preparation of MOF-199 and CuO

In a typical procedure, 1.7 g of $CuCl_2.2H_2O$ was dissolved in 150 ml of water/ethanol/DMF solvent mixture (1/1/1 ratio) under ultrasound for 30 min. Next, 2.8 g of H_3BTC was added to the copper salt solution, and the mixture was sonicated for 10 min. The intermittent microwave reaction was carried out for 60 minutes (20 seconds running, 10 seconds off) with a temperature control of 60 °C. MOF-199 was collected after centrifugation, washing, and drying at 60 °C overnight. Microwave-synthesized Cu-BTC is calcined in ambient air at a temperature range of 200 - 700 °C. The heating time was set to 2 hours with a heating rate of 10 °C/min.

2.3. Characterization of materials

The phase structure of the sample was examined by X-ray diffraction (XRD PANalytical X′ Pert Powder, Netherlands) using Cu Kα radiation. The scanning electron microscope characterized the microstructure and morphology (SEM HITACHI S-4800). The chemical states and compositions of the sample were performed by energy-dispersive X-ray spectroscopy with mapping (EDX, HITACHI S-4800). The Brunauer–Emmett–Teller (BET) specific surface area and porosity of the samples were determined by nitrogen adsorption-desorption (NOVATouch LX2, QUANTACHROME, USA) at 77 K. Thermal gravimetric analysis (TGA/DTG NETZSCH STA 409 PC/PG, Germani) investigated the sample's thermodynamic property.

III. RESULT AND DISCUSSION

3.1. Characteristics of Cu-BTC

The morphology and structure of microwave-synthesized Cu-BTC were characterized by scanning electron microscopy imaging. The SEM image (Fig. 1 a&b) shows that the obtained Cu-BTC has an octahedral shape with 20-30 nm dimensions.

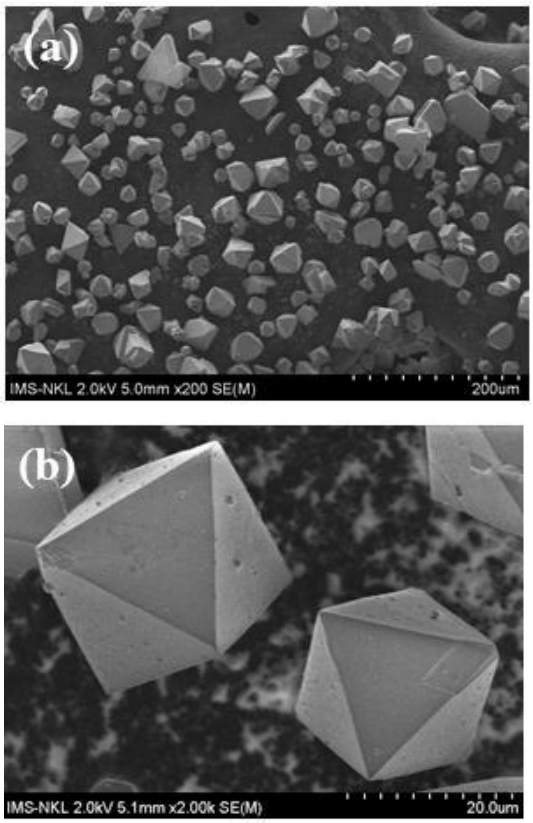

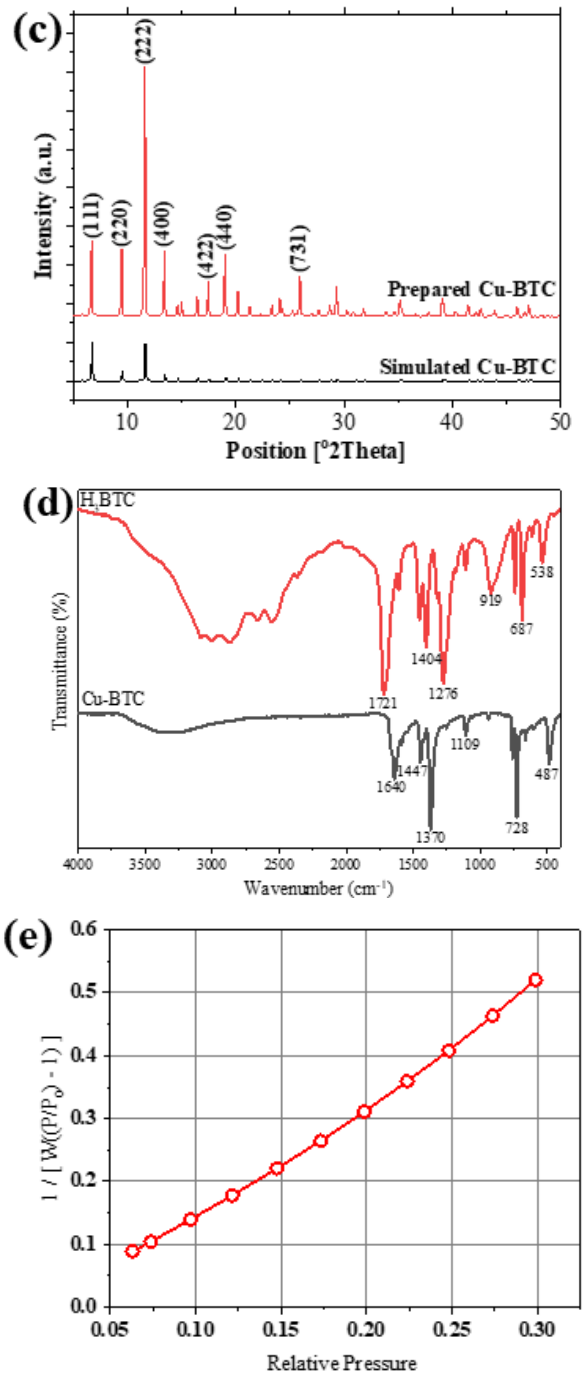

Fig .1: SEM images of the prepared Cu-BTC (a, b); XRD pattern of simulated and prepared Cu-BTC (c); FTIR spectrum of H3BTC and Cu-BTC (d); the BET diagram of the prepared Cu-BTC (e).

The BET surface area of the material was found to be 1,059 m^2/g. XRD test was performed (Fig 1c), and the diffraction pattern of the prepared sample was in good agreement with the simulated ones, indicating the formation of high-purity Cu-BTC [42]. FTIR was used to study the Cu-BTC bond properties further. As shown in Fig. 1d, the absorption band at 1721 cm^{-1} corresponding to

protonated ligands disappeared in the spectrum of Cu-BTC, indicating complete deprotonation of H3BTC after the reaction. On the other hand, two characteristic bands at 1404 cm^{-1} and 1276 cm^{-1} assigned to the stretching vibrations of carboxylate groups were observed in Cu-BTC. At 728 cm^{-1}, it is assigned the CH bond of the benzene ring, and the Cu-O bond forms between the carboxylic groups of H_3BTC and Cu(II) [42].

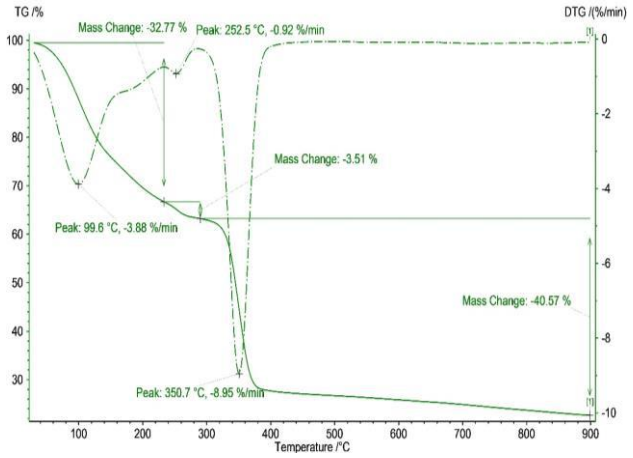

Fig. 2: The TG/DTG curve of the prepared Cu-BTC.

TG/DTG was used to test the microwave-synthesized Cu-BTC framework's thermal stability and thermal decomposition limit. As seen in Fig. 2, CuBTC begins to lose weight below 250 °C due to the evaporation of guest H_2O molecules physically adsorbed in the MOF. The minimum of the DTG diagram appearing at 99.6 °C is assigned to the phase transition point of H_2O. After that, a stable temperature occurs in the range of 250-350 °C, corresponding to two minima on the DTG diagram at 252.5 °C and 350.7 °C of the organic junction transformation in the framework. Next, the TG pattern increases sharply as the temperature rises due to the thermal decomposition of the BTC ligands in the frameworks. After 400 °C, the organic ligand has been wholly oxidized, and the resulting product is the remaining inorganic part. Thermal analysis results are the basis for choosing the calcination temperature for creating pure porous CuO.

3.2. Characteristics of pure porous CuO

Based on the TG thermal analysis results, the calcination temperature was selected from 250 °C to 700 °C. As shown in Figure 3, the sample calcined at 250 °C still retains the diffraction peaks of MOF-199. Diffraction peaks of CuO appear in calcined MOF-199 samples at calcination temperatures of 300 °C or higher. At different calcination temperatures, the peak intensities in the samples are different. Among the investigated temperatures, the diffraction pattern of the sample calcined at 550 °C has the highest peak intensity. The results show that CuO produced from MOF-199 at this temperature has the best crystallinity.

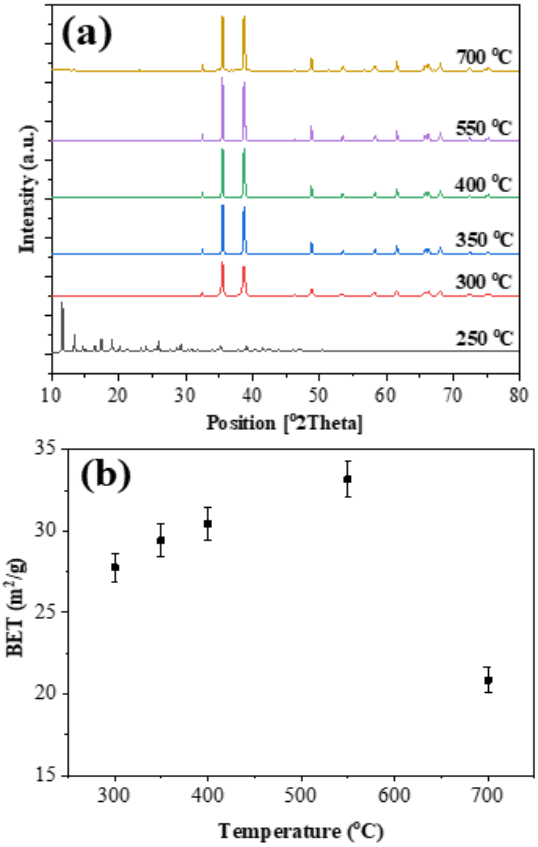

Fig.3: XRD patterns (a) and BET (b) values of calcined MOF-199 samples.

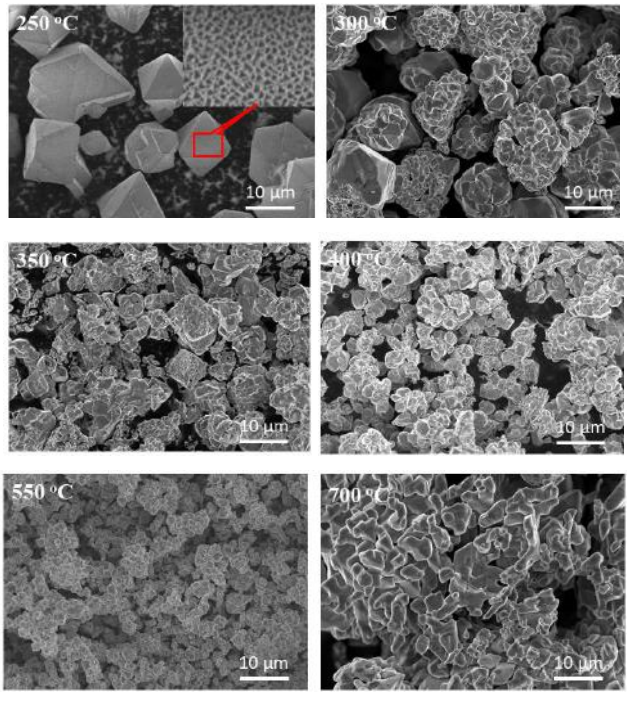

Fig. 4: The SEM of calcined MOF-199 samples.

The surface area of the prepared CuO samples was determined by N_2 isotherm adsorption measurement and is shown in Fig. 3b. The BET value showed a slight increase when the calcination temperature was increased. Still, it decreased suddenly when the calcination temperature rose to 700 °C. The hypothesis is that the porous framework collapses when the temperature increases and the crystal structure of CuO is also poorer.

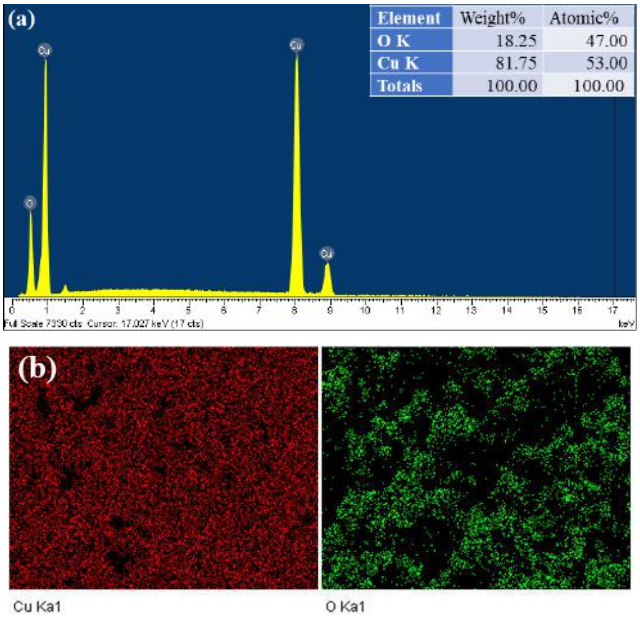

Fig. 5: EDX spectra (a) and mapping images (b) of CuO-derivated MOF-199 at 550 °C.

The morphology and size of MOF-199 calcined at different temperatures are shown in Figure 4. SEM images show an evident change in the crystal structure of Cu-BTC according to calcination temperature. At 250 °C, the metal-organic framework structure remained intact. However, there were signs of thermal impact on the bond framework, leading to the destruction of the crystal surface. Samples calcined at 300 ºC showed separation of grains from the framework but retained the original framework's morphology. Some particles have not been effectively affected by heat on their structures. When increasing the calcination temperature to 350 °C and 400 °C, CuO particles begin to form and leave the frame structure. The sample calcined at a higher temperature (550 °C) produced particles of uniformly small size. According to the calculation results, this sample has the highest surface area (Fig. 3b) and sharpest crystallinity (Fig. 3a). However, when the calcination temperature reaches 700 °C, CuO particles tend to agglomerate to create more giant cubes. Although the melting temperature of CuO is more than 1300 °C, CuO formed from the heating process of MOF-199, which breaks the framework at a temperature lower than the melting temperature, can still solidify. This phenomenon affects the crystalline properties and other characteristics of CuO produced at this temperature. This result coincides with published research on the recrystallization annealing temperature for CuO [27].

The EDX spectrum and mapping image of CuO prepared at 550 °C, shown in Figure 5 (a&b), show that only two elements in the sample (Cu and O) are uniformly distributed. This result demonstrates the purity of CuO when made from MOF-199 by calcination in air. The atomic ratio in the compound also shows nCu/nO ~ 1/1, consistent with the molecular formula of CuO.

IV. CONCLUSION

Copper(II) oxide was prepared from the copper 1,3,5-benzene tricarboxylate framework by calcination in ambient air. The resulting CuO has uniform size and morphology within the 1-2 um range at a calcination temperature of 550 °C. The surface area of CuO reaches 33.16 m^2/g, higher than some results of manufacturing CuO by methods and other materials. The research results are the basis for applying CuO produced by the MOF-199 calcination method for advanced oxidation catalysis in treating organic gases and vapors.

ACKNOWLEDGEMENTS

This research is funded by the Department of Inorganic Materials, Institute of Chemistry and Materials.

REFERENCES

[1] Liu, K.-G.; Bigdeli, F.; Panjehpour, A.; Hwa Jhung, S.; Al Lawati, H. A. J.; Morsali, A (2023). Potential applications of MOF composites as selective membranes for separation of gases. *Coordination Chemistry Reviews*, *496*, 215413. doi: 10.1016/j.ccr.2023.215413

[2] Mehri Lighvan, Z.; Hosseini, S. R.; Norouzbahari, S.; Sadatnia, B.; Ghadimi, A. (2023). Synthesis, characterization, and selective gas adsorption performance of hybrid NH2-MIL-101(Fe)/ZIF-8 metal organic framework (MOF). *Fuel, 351(5),* 128991. doi: 10.1016/j.fuel.2023.128991

[3] Tao, Y. R.; Xu, H. J. (2024). A critical review on potential applications of Metal-Organic frameworks (MOFs) in adsorptive carbon capture technologies. *Applied Thermal Engineering, 236(Part A),*121504. doi: 10.1016/j.applthermaleng.2023.121504

[4] Shi, X.; Lee, G. A.; Liu, S.; Kim, D.; Alahmed, A.; Jamal, A.; Wang, L.; Park, A.-H. A. (2023). Water-stable MOFs and hydrophobically encapsulated MOFs for CO2 capture from ambient air and wet flue gas. *Materials Today*, *65*, 207-226. doi: 10.1016/j.mattod.2023.03.004.

[5] Zhang, Y.; Liu, H.; Gao, F.; Tan, X.; Cai, Y.; Hu, B.; Huang, Q.; Fang, M.; Wang, X. (2022). Application of

MOFs and COFs for photocatalysis in CO_2 reduction, H_2 generation, and environmental treatment. *EnergyChem, 4* (4), 100078. doi: 10.1016/j.enchem.2022.100078.

[6] Poonia, K.; Patial, S.; Raizada, P.; Ahamad, T.; Parwaz Khan, A. A.; Van Le, Q.; Nguyen, V. H.; Hussain, C. M.; Singh, P. (2023). Recent advances in Metal Organic Framework (MOF)-based hierarchical composites for water treatment by adsorptional photocatalysis: A review. *Environ Res, 222*, 115349. doi: 10.1016/j.envres.2023.115349

[7] Liu, X.; Shan, Y.; Zhang, S.; Kong, Q.; Pang, H. (2023). Application of metal organic framework in wastewater treatment. *Green Energy & Environment, 8* (3), 698-721. doi: 10.1016/j.gee.2022.03.005

[8] Yan, D.; Li, M. (2023). Stearic acid-modified MOF-based composite phase change materials for solar-thermal energy conversion and storage. *Solar Energy, 262*, 111843. doi: 10.1016/j.solener.2023.111843

[9] Dai, Y.; Zhang, G.; Peng, Y.; Li, Y.; Chi, H.; Pang, H. (2023). Recent progress in 1D MOFs and their applications in energy and environmental fields. *Advances in Colloid and Interface Science, 321*, 103022. doi: 10.1016/j.cis.2023.103022

[10] Hu, X.; Zheng, W.; Wu, M.; Chen, L.; Chen, S. (2023), Composites of metal-organic frameworks (MOFs) and LDHs for energy storage and environmental applications: Fundamentals, progress, and perspectives. *Sustainable Materials and Technologies, 37*, e00691. doi: 10.1016/j.susmat.2023.e00691

[11] Sun, Y.; Jiang, X.; Liu, Y.; Liu, D.; Chen, C.; Lu, C.; Zhuang, S.; Kumar, A.; Liu, J. (2021). Recent advances in Cu(II)/Cu(I)-MOFs based nano-platforms for developing new nano-medicines. *J Inorg Biochem, 225*, 111599. doi: 10.1016/j.jinorgbio.2021.111599

[12] Le Thanh, B.; Nguyen Thi, H. P.; La Duc, D.; Nguyen Thi, P. (2021). Green synthesis of MIL-100(Fe) metal-organic frameworks as a carrier for chloroquine delivery. *Journal of Military Science and Technology, 76* (12), 61-67. doi: 10.54939/1859-1043.j.mst.76.2021.61-67

[13] Le B. T.; Nguyen C. Q.; Nguyen P. T.; Ninh H. D.; Le T. M.; Nguyen P. T. H.; D., L. D. (2022). Fabrication of Porous Fe-Based Metal-Organic Complex for the Enhanced Delivery of 5-Fluorouracil in In Vitro Treatment of Cancer Cells. *ACS Omega, 7*(50), 46674-46681. doi: 10.1021/acsomega.2c05614

[14] Patel, N. B.; Vala, N.; Shukla, A.; Neogi, S.; Mishra, M. K. (2023). Catalytic activity of Cu-BTC metal organic framework for borrowing hydrogen and tandem reactions of an alcohol under solvent and base free condition. *Inorganica Chimica Acta, 554*, 121546. doi: 10.1016/j.ica.2023.121546

[15] Peedikakkal, A. M. P.; Aljundi, I. H. (2020). Mixed-Metal Cu-BTC Metal-Organic Frameworks as a Strong Adsorbent for Molecular Hydrogen at Low Temperatures. *ACS Omega, 5* (44), 28493-28499. doi: 10.1021/acsomega.0c02810

[16] Ho, P. S.; Chong, K. C.; Lai, S. O.; Lee, S. S.; Lau, W. J.; Lu, S.-Y.; Ooi, B. S. (2022). Synthesis of Cu-BTC Metal-Organic Framework for CO2 Capture via Solvent-free Method: Effect of Metal Precursor and Molar Ratio. *Aerosol and Air Quality Research, 22 (12)*. 220135. doi: 10.4209/aaqr.220235

[17] Zhao, T.; Nie, S.; Luo, M.; Xiao, P.; Zou, M.; Chen, Y. (2024). Research progress in structural regulation and applications of HKUST-1 and HKUST-1 based materials. *Journal of Alloys and Compounds, 974*, 172897. doi: 10.1016/j.jallcom.2023.172897

[18] Mazani, M.; Aghapour Aktij, S.; Rahimpour, A.; Tavajohi Hassan Kiadeh, N. (2019). Cu-BTC Metal−Organic Framework Modified Membranes for Landfill Leachate Treatment. *Water, 12* (1). 91. doi: 10.3390/w12010091

[19] Venu, B.; Shirisha, V.; Vishali, B.; Naresh, G.; Kishore, R.; Sreedhar, I. (2020). Venugopal, A., A Cu-BTC metal–organic framework (MOF) as an efficient heterogeneous catalyst for the aerobic oxidative synthesis of imines from primary amines under solvent free conditions. *New Journal of Chemistry, 44* (15), 5972-5979. doi: 10.1039/C9NJ05997K

[20] Li, C.; Wu, K. (2021). Cu-BTC frameworks based electrochemical sensor for hazardous malachite green in aquaculture. *Anal Chim Acta, 1162*, 338473. doi: 10.1016/j.aca.2021.338473

[21] Yang, J.; Yuling, L.; Penghe, Z.; Hao, S.; Chuanchuan, D.; Ruihao, S.; Feifei, L. (2022). Chemical thermodynamic and catalytic mechanism analysis of Cu-BTC-derived CuOx/C catalyst for selective catalytic reduction (SCR). *Molecular Catalysis, 531*. 112710. doi: 10.1016/j.mcat.2022.112710

[22] Huang, P.; Lei, J.; Sun, Z.; Hu, X. (2021), Fabrication of MOF-derivated CuOx-C electrode for electrochemical degradation of ceftazidime from aqueous solution. *Chemosphere, 268*, 129157. doi: 10.1016/j.chemosphere.2020.129157

[23] Ding, Y.; Guo, X.; Liang, C.; Wu, Z.; Meng, G.; Zang, Z.; He, Y. (2022). Temperature modulated p-n transition NO2 sensor in metal-organic framework-derived CuO. *Sensors and Actuators B: Chemical, 359*. 131605. doi: 10.1016/j.snb.2022.131605

[24] Gu, C.; Wang, Q.; Zhang, L.; Yang, P.; Xie, Y.; Fei, J. (2020). Ultrasensitive non-enzymatic pesticide electrochemical sensor based on HKUST-1-derived copper oxide @ mesoporous carbon composite. *Sensors and Actuators B: Chemical, 305*. 127478. doi: 10.1016/j.snb.2019.127478

[25] He, L.; Liu, J.; Yang, L.; Song, Y.; Wang, M.; Peng, D.; Zhang, Z.; Fang, S. (2018), Copper metal–organic framework-derived CuOx-coated three-dimensional reduced graphene oxide and polyaniline composite: Excellent candidate free-standing electrodes for high-performance supercapacitors. *Electrochimica Acta, 275*, 133-144. doi: 10.1016/j.electacta.2018.04.089

[26] Saleem, S.; Jabbar, A. H.; Jameel, M. H.; Rehman, A.; Kareem, Z. H.; Abbas, A. H.; Ghaffar, Z.; Razzaq, S. A.; Pashameah, R. A.; Alzahrani, E.; Ng, E.-P.; Sapuan, S. M. (2022), Enhancement in structural, morphological, and optical properties of copper oxide for optoelectronic device applications. *Nanotechnology Reviews, 11* (1), 2827-2838. doi: 10.1515/ntrev-2022-0473

[27] Sivayogam, D.; Kartharinal Punithavathy, I.; Johnson Jayakumar, S.; Mahendran, N. (2022). Study on structural, electro-optical and optoelectronics properties of CuO nanoparticles synthesis via sol gel method. *Materials Today: Proceedings, 48(part 2)*, 508-513. doi: 10.1016/j.matpr.2021.04.494

[28] Hoàng, T. H. H.; Đào, N. N. (2014). Characteristics and catalytic activity for the CO oxidation reaction of CuO, CeO_2 oxides and CuO-CeO_2 mixed oxides. *Journal of Chemistry, 52* (1), 86-90. doi:

[29] Nguyen, T. T. T.; Nguyen, Y. N. N.; Tran, X. T.; Nguyen, T. T. T.; Tran, T. V. (2023). Green synthesis of CuO, ZnO and CuO/ZnO nanoparticles using Annona glabra leaf extract for antioxidant, antibacterial and photocatalytic activities. *Journal of Environmental Chemical Engineering, 11* (5). 111003. doi: 10.1016/j.jece.2023.111003

[30] Jadhav, A. L.; Jadhav, S. L.; Mandlekar, B. K.; Kadam, A. V. (2023). Hydrothermally synthesized three-dimensional hierarchical CuO nanomaterials for energy storage applications. *Materials Chemistry and Physics, 310*. 128494. doi: 10.1016/j.matchemphys.2023.128494

[31] Dai, X.; Fang, X.; Wu, H. (2024). Highly sensitive and selective room-temperature NO sensor based on rich-oxygen vacancy CuO nanoflakes. *Materials Letters, 356*. 135564. doi: 10.1016/j.matlet.2023.135564

[32] Ye, Y.; Xu, J.; Gao, L.; Zang, S.; Chen, L.; Wang, L.; Mo, L. (2023). CuO/CeO_2 catalysts prepared by modified impregnation method for ethyl acetate oxidation. *Chemical Engineering Journal, 471*. 144667. doi: 10.1016/j.cej.2023.144667

[33] Shen, Z.; Xing, X.; Wang, S.; Lv, M.; Zheng, Z.; Li, J.; Li, H. (2023). High activity of CuO/#-Fe2O3 for low temperature CO oxidation: Effect of support crystal types in catalyst design. *Journal of the Energy Institute, 110*, 101339. dọi: 10.1016/j.joei.2023.101339

[34] Yun, J.; Wu, L.; Hao, Q.; Teng, Z.; Gao, X.; Dou, B.; Bin, F. (2022). Non-equilibrium plasma enhanced oxygen vacancies of CuO/CeO_2 nanorod catalysts for toluene oxidation. *Journal of Environmental Chemical Engineering, 10 (3).* 107847. doi: 10.1016/j.jece.2022.107847

[35] Dorner, L.; Cancellieri, C.; Rheingans, B.; Walter, M.; Kagi, R.; Schmutz, P.; Kovalenko, M. V.; Jeurgens, L. P. H. (2019). Cost-effective sol-gel synthesis of porous CuO nanoparticle aggregates with tunable specific surface area. *Sci Rep, 9 (1)*, 11758. doi: 10.1038/s41598-019-48020-8

[36] Anitha, T. V.; Gadha Menon, K.; Venugopal, K.; Vimalkumar, T. V. (2024). Investigating the role of film thickness on the physical properties of sol-gel coated CuO thin films: Discussing its potentiality in optoelectronic applications. *Materials Science and Engineering: B, 299*, 116960. doi: 10.1016/j.mseb.2023.116960

[37] Abdel-Galil, A.; Moussa, N. L. (2023). Nanostructure CuO thin film deposited by spray pyrolysis for technological applications. *Radiation Physics and Chemistry, 212*. 111119. doi: 10.1016/j.radphyschem.2023.111119

[38] Mahana, D.; Mauraya, A. K.; Singh, P.; Muthusamy, S. K. (2023). Evolution of CuO thin films through thermal oxidation of Cu films prepared by physical vapour deposition techniques. *Solid State Communications*, 366-367, 115152. doi: 10.1016/j.ssc.2023.115152

[39] Kongvarhodom, C.; Nammahachak, N.; Tippomuang, W.; Fongchaiya, S.; Turner, C.; Ratanaphan, S. (2021). Role of crystallographic textures on the growth of CuO nanowires via thermal oxidation. *Corrosion Science, 193*, 109898. doi: 10.1016/j.corsci.2021.109898

[40] Warsi, A.-Z.; Hussien, O. K.; Iftikhar, A.; Aziz, F.; Alhashmialameer, D.; Mahmoud, S. F.; Warsi, M. F.; Saleh, D. I. (2022). Co-precipitation assisted preparation of Ag_2O, CuO and Ag_2O/CuO nanocomposite: Characterization and improved solar irradiated degradation of colored and colourless organic effluents. *Ceramics International, 48 (13)*, 19056-19067. doi: 10.1016/j.ceramint.2022.03.194

[41] Banu, T.; Jamal, M.; Gulshan, F. (2023). Opto-structural properties and photocatalytic activities of CuO NPs synthesized by modified sol-gel and Co-precipitation methods: A comparative study. *Results in Materials, 19*, 100419. doi: 10.1016/j.rinma.2023.100419

[42] Garg, D.; Rekhi, H.; Kaur, H.; Singh, K.; Malik, A. K. (2022). A Novel Method for the Synthesis of MOF-199 for Sensing and Photocatalytic Applications. *J Fluoresc, 32 (3)*, 1171-1188. doi: 10.1007/s10895-022-02902-9